STUDY OF HYDRODYNAMICS AND CONJUGATE HEAT EXCHANGE ON THE STABILIZATION SECTION IN THE FLOW OF A HEAT CARRIER IN A BUNDLE OF FINNED TUBES

A. A. Mikhalevich, V. A. Nemtsev, V. I. Nikolaev, and L. N. Shegidevich

UDC 536.24

A conjugate problem of heat exchange and hydrodynamics in a channel of complex shape is numerically solved.

The present article examines hydrodynamics and heat exchange in the stabilization section of a forced laminar flow of a heat carrier in a channel formed by a longitudinally finned bundle of tubes arranged triangularly. Since experimental study of such problems is associated with certain technical difficulties, we will resort to numerical modeling of the hydrodynamics and heat transfer on the basis of a three-dimensional mathematical model. A solution is obtained by the finite element method. Here, the sought quantity is represented by a discrete model defined by trial functions at the nodes of the elements comprising the modeled region [1]. Galerkin's modification was used to obtain the solution. The use of this approach in combination with the finite-element model was examined in [2, 3].

The region investigated is shown in Fig. 1 and represents an elementary symmetry cell ABCD formed by symmetry lines AB, BC, CD, and part of the inside surface of the tube. We took 12 [4] for the number of fins on one tube. Secondary flows were not considered, and we assumed that the heat carrier is incompressible. Then the system of differential conservation equations in the boundary-layer approximation has the form:

$$\rho U \frac{\partial U}{\partial z} = \frac{\partial}{\partial x}\left(\mu \frac{\partial U}{\partial x}\right) + \frac{\partial}{\partial y}\left(\mu \frac{\partial U}{\partial y}\right) - \frac{\partial P}{\partial z}; \tag{1}$$

$$\rho U c_p \frac{\partial T}{\partial z} = \frac{\partial}{\partial x}\left(\lambda \frac{\partial T}{\partial x}\right) + \frac{\partial}{\partial y}\left(\lambda \frac{\partial T}{\partial y}\right); \tag{2}$$

$$\frac{\partial^2 T}{\partial x^2} + \frac{\partial^2 T}{\partial y^2} = 0; \tag{3}$$

$$\rho U S = \text{const}; \tag{4}$$

$$U|_{\Gamma_1} = 0, \quad \left.\frac{\partial U}{\partial n}\right|_{\Gamma_2} = 0; \tag{5}$$

$$T_{R_{\text{in}}} = T_R, \quad \left.\frac{\partial T}{\partial n}\right|_{\Gamma_2} = 0; \tag{6}$$

$$T_{R_{\text{out}}-0} = T_{R_{\text{out}}+0}, \quad \lambda_{\text{wa}} \left.\frac{\partial T}{\partial n}\right|_{R_{\text{out}}-0} = \lambda_c \left.\frac{\partial T}{\partial n}\right|_{R_{\text{out}}+0}, \tag{7}$$

where (1)-(3) are the equations of motion and energy for the intertube region and the heat-conduction equation for the region of the finned tube proper. The system is closed by continuity equation (4), boundary conditions (5) and (6), and compatibility conditions (7).

It should be noted that, in the numerical solution, we allowed for the possible use of polar and cylindrical coordinates, as well as for a mutual transition from one type of coordinates to another. Both linear and quadratic tetragonal elements were used in the machine realization of the method. The fact that the latter may have curved surfaces as its boundaries makes it particularly convenient for studying curved regions. There is a signifi-

Institute of Nuclear Power, Academy of Sciences of the Belorussian SSR, Minsk. Translated from Inzhenerno-Fizicheskii Zhurnal, Vol. 46, No. 2, pp. 185-189, February, 1984. Original article submitted October 5, 1982.

 0022-0841/84/4602-0130$08.50© 1984 Plenum Publishing Corporation

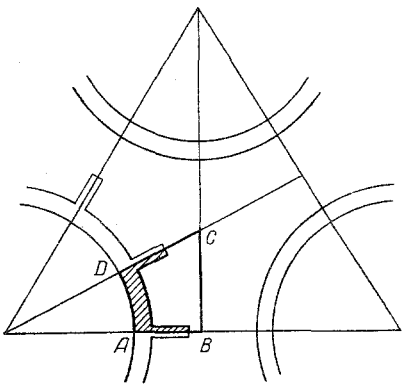

Fig. 1

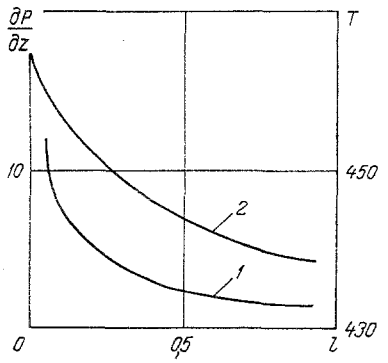

Fig. 2

Fig. 1. Elementary symmetry cell ABCD for the investigated conjugate region: solid wall — free flow.

Fig. 2. Distribution of the pressure gradient and cross-sectional mean temperature along the channel with the following inlet parameters: U_{in} = 0.2 m/sec; T_{in} = 473°K; T_{wa} = 423°K. 1, 2) Curves for the pressure gradient and the cross-sectional mean temperature. $\partial P/\partial z$, Pa/m; l, m.

cant time savings in preparing the initial data when using complex elements. Moreover, comparison of the results [3] shows that, given the same number of degrees of freedom, use of complex elements improves accuracy considerably. The optimum number of elements into which to divide the region was chosen as a result of a numerical experiment. The method of trial functions [5] was used to check the numerical scheme.

The computing procedure was constructed on the basis of the method of successive approximations. Here, we used Bergstein's modification, ensuring rapid convergence. As the zeroth approximation, we assigned a flat velocity and temperature profile at the channel inlet. We then constructed the following iteration scheme:

$$U^{(0)} \to \bar{\tau}_w \to \frac{\partial P}{\partial z} \to U^{(1)}. \tag{8}$$

The convergence condition of the process was satisfaction of the continuity equation (4). The shear stresses on the wall were determined as follows:

$$\bar{\tau}_w = \frac{1}{l}\int_0^l \tau_w \, dl, \tag{9}$$

$$\tau_w = \mu \frac{\partial U}{\partial n}. \tag{10}$$

The total pressure drop due to inertial forces and friction on the wall is equal to [6]:

$$\frac{\partial P}{\partial z} = \frac{\Pi}{S_{chn}} \bar{\tau}_w + \rho U \frac{\partial U}{\partial z}. \tag{11}$$

Numerical study of the hydrodynamics of the inlet section of the channel yielded the pressure-gradient distribution along the channel, the distribution of local velocities in characteristic sections of the symmetry cell ABCD, and the shear stresses on the washed part of the channel perimeter.

Figure 2 shows the change in the pressure gradient and the cross-sectional mean temperature in the stabilization section in the case of simultaneous formation of the hydraulic and thermal boundary layers. The highest pressure gradients are reached at the inlet. They then decrease and become constant at the end of the stabilization section.

Figure 3 shows the change in the velocity profile in the channel section as the boundary layer is formed. It is apparent that, in the section close to the inlet, located at z_k = 0.05 m, velocity remains nearly unchanged. Then, with increasing distance from the inlet, the profile becomes more and more parabolic until a stable value is reached. Figure 3 shows the

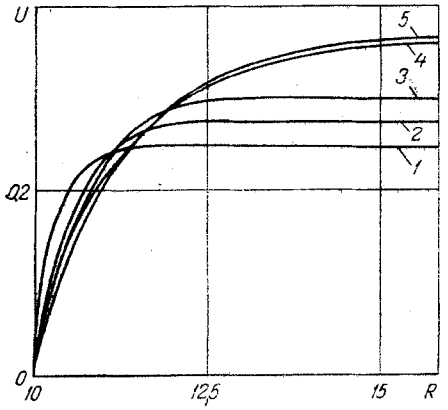

Fig. 3

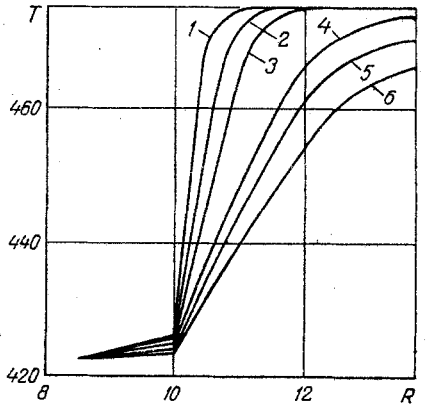

Fig. 4

Fig. 3. Radial velocity profiles in channel sections for the angle $\varphi = 15°$ and $n_f = 12$: 1-5) curves for the values $z_k = 0.05$, 0.1, 0.3, 0.8, and 0.95 m, respectively. U, m/sec; R, mm.

Fig. 4. Radial distributions of local temperatures for the angle $\varphi = 15°$ with the following inlet parameters: $T_{in} = 473°K$, $T_{wa} = 423°K$, $U_{in} = 0.2$ m/sec: 1-6) curves for $z_k = 0.01$, 0.05, 0.2, 0.4, 0.6, and 0.85, respectively. T, °K.

distribution for different values of the angle φ, i.e., for different characteristic channel sections. Certain qualitative conclusions on the character of heat exchange in the tube bundles can be made from the pattern of velocity distribution. For example, stagnant zones with a reduced flow velocity are located in the intertube region, and these zones may lead to local overheating of the tube surface.

Figure 4 graphically represents the formation of the temperature profile in the finned-wall – free-flow conjugate region. The curves were constructed for characteristic directions in the investigated region, i.e., for different values of the angle φ.

The results shown in the figures were obtained with boundary conditions of the first kind, although it should be noted that the algorithm makes it possible to assign conditions of the second and third kinds, as well as mixed boundary conditions. The solutions presented here were obtained for a triangular array of tubes with a spacing equal to 1.3.

The numerical results obtained with the above model were compared with test results in [7], and results of an electrical modeling [8]. Since at present the literature contains data only for unfinned channels of a similar geometry [7] and for stabilized flow, these variants were modeled, and the results of the comparison proved satisfactory. We also modeled the experiment in [9] for the stabilization section in a circular tube to check the solutions for the initial section. Here, the discrepancy between the experimental and theoretical parameters ranged from 1 to 3%.

The good agreement between the theoretical and experimental data confirms the correctness of the mathematical model of the physical process, the correctness of the assumptions made, and the effectiveness of the finite elements method in solving problems of this class.

The three-dimensional mathematical model and program developed make it possible to calculate the hydrodynamics and heat exchange in different heat exchangers with smooth and finned surfaces with allowance for the sections of hydrodynamic and thermal stabilization.

NOTATION

ρ, density of the heat carrier; λ_{wa}, thermal conductivity of the wall; λ_c, thermal conductivity of the heat carrier; c_p, specific heat of the heat carrier; μ, absolute viscosity of the heat carrier; U, velocity of the heat carrier; T, temperature; x, y, z, Cartesian coordinates; P, pressure; R_{in}, internal radius of the tube; R_{out}, external radius of the tube; T_{wa}, temperature of the tube wall surface; Γ_1, contour of the washed perimeter of the tube; Γ_2, lines of symmetry of the cell ABCD; n, vector of the normal to the symmetry lines; T_{in}, temperature of the heat carrier at the channel inlet; U_{in}, mean velocity at the inlet; z_k, spacing along the z axis along the channel; Π, perimeter of the washed part of the channel; S_{chn}, cross-sectional area of the investigated symmetry cell; n_f, number of fins on the tube.

LITERATURE CITED

1. L. Sigerlind, Use of the Finite Element Method [Russian translation], Mir, Moscow (1979).
2. J. Conner and K. Brebbia, Finite Element Method in Fluid Mechanics [Russian translation], Sudostroenie, Leningrad (1979).
3. O. Zenkevich, Finite Element Method in Engineering [Russian translation], Mir, Moscow (1975).
4. Yu. P. Vorob'ev, N. V. Zezyulya, V. U. Lemeshev, et al., "Effectiveness of finning in a chemically reactive heat carrier," in: Dissociating Gases as Heat Carriers and Working Substances in Power Plants [in Russian], Part 2, ITMO, Minsk (1973), pp. 194-202.
5. A. A. Samarskii, Introduction to the Theory of Difference Methods [in Russian], Nauka, Moscow (1971).
6. B. S. Petukhov, L. G. Genin, and S. A. Kovalev, Heat Exchange in Nuclear Power Plants [in Russian], Atomizdat, Moscow (1974).
7. V. E. Minashin, A. A. Sholokhov, and Yu. I. Gribanov, Thermophysics of Nuclear Reactors with Liquid-Metal Cooling and Methods of Electrical Modeling [in Russian], Atomizdat, Moscow (1971).
8. V. A. Nemtsev and V. I. Nikolaev, "Study of hydrodynamics and heat exchange in laminar flow about tubes with longitudinal fins by the method of electrohydrodynamic analogy," Izv. Akad. Nauk BSSR, Ser. FEN, No. 1, 79-83 (1982).
9. Ma-Tin-Ji, Development of Heat Transfer in Tubes with Laminar Flow [Russian translation], Izv. Akad. Nauk SSSR, Moscow (1962), pp. 27-42.

PHYSICAL FEATURES OF THE EVAPORATIVE LIQUID COOLING OF A POROUS METAL—CERAMIC FUEL ELEMENT

V. A. Maiorov and L. L. Vasil'ev

UDC 536.24:532.685

This article compares calculated data with results of an experimental study of the temperature field of a porous metal—ceramic fuel element during its evaporative liquid cooling and reports physical features of this process.

The study [1] showed analytically that the evaporation of a liquid flow inside a porous heated metal is characterized by a limiting high rate of heat transfer. The literature presently does not have the empirical data needed to back up this theoretical finding. For example, the small thickness of the porous plates used in the well-known study [2] does not provide an evaporation region inside the porous metal in the two-phase-flow discharge regime which is long enough to measure temperature, and there is no possibility of stable operation in the regime of superheated-vapor discharge.

Presented below is empirical data on the cooling of porous stainless-steel specimens in the form of rectangular bars 10 × 16 × 125 mm by distilled water. The bars are heated by a direct electrical current. The study [3] described the specimens and the results of investigation of the structure of the outgoing two-phase flow and the temperature field on the outer surface. The temperature through the specimen thickness was measured at two stations along the bar. Here, thermocouples were embedded into channels drilled along a normal to the lateral surface on one side. These channels were drilled to the middle of the bar. The distorting effect of the channels on the flow of coolant and the temperature field was reduced by displacing them alternately 2-3 mm heightwise in the direction of the cross section of interest. With a constant coolant discharge, we gradually increased the power supplied to the specimen. We began with the regime of discharge of a subheated (relative to boiling)

Novolipetsk Polytechnic Institute. A. V. Lykov ITMO, Academy of Sciences of the Belorussian SSR. Translated from Inzhenerno-Fizicheskii Zhurnal, Vol. 46, No. 2, pp. 189-195, February, 1984. Original article submitted November 3, 1982.

 © 1984 Plenum Publishing Corporation